

# Cascaded Fractional Kalman Filtering for State and Current Estimation of Large-Scale Lithium-Ion Battery Packs

Martin Kupper<sup>1,2</sup>, Jochen Brenneisen<sup>1</sup>, Oliver Stark<sup>1</sup>, Stefan Krebs<sup>1</sup> and Sören Hohmann<sup>1</sup>

1. Institute of Control Systems, Karlsruhe Institute of Technology, Karlsruhe, Germany  
E-mail: martin.kupper@kit.edu

2. ITK Engineering GmbH, Rülzheim, Germany

**Abstract:** In this paper, a cascaded fractional Kalman filter for state of charge and branch current estimation of large-scale battery systems is proposed. As a centralized approach for the estimation of a large-scale system is costly in terms of effort and time, a partition into smaller and, therefore, simpler subsystems is applied. Since the overall system is divided into smaller units, a local computation is allowed and complexity reduced. In these distributed systems, usually, the subsystems communicate with each other to exchange relevant data. Using a model based on mesh currents, we receive a cascaded system structure which results in a hierarchical arrangement of all subsystems. This concludes in a one-directional information flow and, therefore, reduces the overall communication effort. Using this proposed approach, it is not only possible to estimate the states of each branch locally but also to calculate the branch currents when the total current is known. Finally, a practical test with real measurement data is presented.

**Key Words:** State of Charge estimation, Current estimation, Kalman filter, Cascaded systems, Fractional order, Battery pack, Large-scale, Lithium-ion

## 1 INTRODUCTION

The state of charge (SOC) is one of the most important variables describing the state of a Lithium-ion battery. As it can not be measured directly it is a central task to accurately estimate present and predict future values. In this paper, we use the most common definition [1] calculating the ratio of remaining electric charge  $Q(t)$  to the rated electric charge  $Q_N$

$$\text{SOC}(t) := \frac{Q(t)}{Q_N}. \quad (1)$$

Being that important, there are various approaches to determine the SOC of a single battery cell [1, 2]. Many applications nowadays are based on models to consider the underlying physical dynamics and to be able to deal with measurement errors [2, 3]. These models are then used as a basis for state estimation.

In recent times, the use of fractional order models was proposed for higher accuracy and a better representation of the physical phenomena of Li-ion cells [4–6]. Using non-integer order differential equations, fractional models describe reality better than conventional models of the same order as they model accurately the internal impedance and the electrochemical dynamics of a battery cell. Hence, they are used more and more frequently in recent time [6–12]. As this model is easy to implement, the additional effort compared to integer order models is negligible and the results are convincing, the application for battery modeling is suitable. Corresponding estimation algorithms have also been proposed with fractional Luenberger-type observers [7] and fractional Kalman Filters [4, 6].

A further challenge for battery systems is to fulfill high power demands, e.g. in electric vehicles. Therefore, a high number of single battery cells are connected in series and in parallel to build a so-called battery pack [13, 14]. As well as for single cells, one of the main tasks is to estimate the SOC of the battery pack. But a difficulty is that mutual effects have to be considered: Due to aging, manufacturing tolerances, temperature differences and different serial connection resistances, some cells are burdened to a different extent than others [15–17]. Following, the single cell's SOC will differ and the SOC of each cell has to be determined separately. The cell currents also have to hold some limits for security and aging reasons, e.g. the maximum peak current specified by the manufacturer. To this, usually, each current has to be measured separately which is costly and causes power losses [2, 18]. To the knowledge of the authors, there are no real-time capable and model-based methods for current estimation of battery packs existent, yet. There exist only few methods, e.g. an iterative algorithm in [19], which is very cost-intensive in terms of computing power and only suitable for simulation purposes, or an approach as in [18] which utilizes a filtered battery terminal voltage for SOC estimation of a single cell without measuring the current, but it does not consider measurement or modelling errors.

One approach for the estimation of a Li-ion battery pack is to use a centralized approach [20]. However, the computation time of a central processor and the process complexity increases for large-scale systems [21].

An alternative way is to split up the overall system into smaller and, therefore, simpler subsystems. Then a single estimation unit can be used for each subsystem which al-

lows a local computation. In such a distributed approach the subsystems communicate with each other to share all necessary variables. The result is usually reduced complexity and sinking computational costs [21]. Such distributed filters have been introduced, e.g. in [21, 22] and have been extended for fractional models in [23].

A special case of a distributed system, using a hierarchical arrangement of subsystems, is a cascaded system. In [24] a distributed Kalman Filter for cascaded systems is proposed. Due to the cascaded system structure an all-to-all communication for transmitting information is not necessary, only a one-directional information flow exists. Therefore, the communication effort compared to a common distributed system is reduced. This cascaded filtering approach has been extended in [25] for fractional order models.

In this paper, we use a nonlinear variable fractional order battery cell model which is extended to a battery pack model. Mesh currents are used to describe the coupling between the particular battery branches. Based on this, a cascaded fractional Kalman filtering approach is used for online and local SOC determination for all cells in each branch. Hereby, the system is split up into subsystems and a cascaded communication procedure is developed which reduces complexity and computational cost due to a reduced order and a local computation. Moreover, this approach does not need to measure every single branch current but can estimate these currents using a mesh current-based model. Since only the total current has to be measured, measurement effort is reduced.

## 2 FRACTIONAL CALCULUS

The most common discrete-time representation of a fractional derivative due to its easy numerical implementation is the definition of Grünwald-Letnikov. Using a variable fractional order, one definition is given in [26] by:

$${}_0D_{t_k}^{\alpha(t_k)} x(t_k) := T^{-\alpha(t_k)} \sum_{j=0}^{k+1} (-1)^j \binom{\alpha(t_k)}{j} x(t_{k+1-j}) \quad (2)$$

where  $D$  is the fractional order derivative,  $\alpha(t_k) \in \mathbb{R}^+$  is the time-variant fractional differentiation order,  $t_k$  is the sampled time and  $T$  is the sampling interval [26].

The summation in (2) respects an infinite number of previous values of  $x$  as  $k$  increases which makes it unsuitable in practice at first glance. Because the binomial coefficient in (2) converges to zero for  $j \rightarrow \infty$ , one can neglect very old values of  $x$ . Therefore, we consider a maximum number  $l$  of past values of  $x$  which is called *short memory principle* (SMP) [25, 27].

The fractional, time-variant, and discrete-time state-space representation can be obtained from (2) following [23, 28] whereby index  $k$  denotes the current time step  $t_k$  in

$$\mathbf{x}_{k+1} = \mathbf{T}^{\alpha_k} \mathbf{f}_k(\mathbf{x}_k, \mathbf{u}_k) + \mathbf{T}^{\alpha_k} \mathbf{w}_k - \sum_{j=1}^z (-1)^j \mathbf{\Gamma}_{j,k} \mathbf{x}_{k+1-j} \quad (3)$$

$$\mathbf{y}_k = \mathbf{g}_k(\mathbf{x}_k, \mathbf{u}_k) + \mathbf{v}_k \quad (4)$$

with

$$\mathbf{\Gamma}_{j,k} := \text{diag} \left[ \binom{\alpha_{1,k}}{j}, \dots, \binom{\alpha_{N,k}}{j} \right] \quad (5)$$

$$\mathbf{T}^{\alpha_k} := \text{diag} [T^{\alpha_{1,k}}, \dots, T^{\alpha_{N,k}}] \quad (6)$$

where  $\mathbf{x}_k \in \mathbb{R}^N$  is the state vector,  $\mathbf{u}_k \in \mathbb{R}^L$  is the input vector,  $\mathbf{y}_k \in \mathbb{R}^M$  is the output vector,  $\mathbf{w}_k \in \mathbb{R}^N$  is the system noise vector,  $\mathbf{v}_k \in \mathbb{R}^M$  is the output noise vector, and  $\alpha_{1,k}, \dots, \alpha_{N,k} \in \mathbb{R}^+$  denote the orders of the fractional derivative at time  $k$  [25, 27]. The upper limit of the sum is denoted by the buffer length  $z = \min(k+1, l)$  due to the SMP. Note that the matrix  $\mathbf{T}^{\alpha_k}$  is often included inside of  $\mathbf{f}_k$  and  $\mathbf{w}_k$  [6].

As the calculation of the states in (3) only by knowing the initial state  $\mathbf{x}_0$  and the sequence of inputs  $(\mathbf{u}_0, \dots, \mathbf{u}_k)$  is not possible because of the theoretical infinite Grünwald-Letnikov sum, it should be noted that  $\mathbf{x}_k$  are not states in the classical sense [29] but rather ‘pseudo-states’. However, for simplicity reasons, in this paper we name  $\mathbf{x}_k$  states. For these states, in fact, an initialization function is needed [30], except one uses an infinite buffer  $z \rightarrow \infty$  which is not possible in practice. As discussed in [25], a fractional order Kalman filter can compensate a missing or wrong initialization of the system. Furthermore, it is discussed in [6] that the initialization of a fractional order state-space model has only a small influence on the SOC estimation of a single cell. Therefore, an exact initialization will be neglected in this paper and the buffer of the cascaded fractional order Kalman filter (CFKF) will be initialized with zeros.

## 3 BATTERY MODEL

### 3.1 Model of a single cell

In this paper, we use the battery model from [6, 8, 11] for a single Li-ion cell of type SLPB 834374H from Kokam. The equivalent circuit model which is used in this paper is shown in Fig. 1. This ‘1-RQ-model’ consists of one single RQ-element, which is composed of a fractional order capacity  $Q$ (SOC) of order  $\alpha$ (SOC) and a parallel connected resistor  $R$ (SOC). The model is completed by an internal resistance  $R_0$ (SOC) and the cell’s open circuit voltage OCV(SOC). It is assumed that the functional relations of the parameters to the SOC are known. The OCV-SOC characteristic of the considered cells including a hysteresis effect is shown in Fig. 2.

As the deviation between the charge and the discharge process is slight the OCV can be approximated by an average curve for moderate and high temperatures in practice [31]. The resulting model is given by the SOC [1, 6]

$$\text{SOC}_{k+1} = \text{SOC}_k + 100 \cdot \frac{\eta \cdot T}{Q_N} \cdot i_{\text{cell},k} + w_{\text{SOC},k} \quad (7)$$

and by the voltages [6]

$$u_{\text{cell},k} = u_{RQ,k} + R_0(\text{SOC}_k) i_{\text{cell},k} + \text{OCV}(\text{SOC}_k) + v_{\text{cell},k} \quad (8)$$

$$u_{RQ,k+1} = \frac{T^{\alpha(\text{SOC}_k)}}{Q(\text{SOC}_k)} \left( i_{\text{cell},k} - \frac{u_{RQ,k}}{R(\text{SOC}_k)} \right) + w_{RQ,k} - \Lambda_{k|z} \quad (9)$$

with

$$\Lambda_{k|z} := \sum_{j=1}^z (-1)^j \binom{\alpha(\text{SOC}_k)}{j} u_{RQ,k+1-j} \quad (10)$$

being an abbreviation for the Grünwald-Letnikov sum for time-step  $k$ , considering the last  $z$  values.  $\text{SOC}_k$  denotes the SOC of the current time step  $k$  and  $i_{cell,k}$  denotes the current of the concerning cell (see Fig. 1). In coincidence with [32] the coulomb efficiency  $\eta$  is assumed to be

$$\eta \approx \begin{cases} 1 & \text{discharging process} \\ 0.992 & \text{charging process.} \end{cases} \quad (11)$$

Putting (7) - (9) in matrix form results in the following non-linear state space structure

$$\begin{aligned} \mathbf{x}_{cell,i,k+1} &:= \begin{pmatrix} \text{SOC}_i \\ u_{RQ,i} \end{pmatrix}_{k+1} \\ &= \begin{pmatrix} \text{SOC}_{i,k} + 100 \cdot \frac{\eta \cdot T}{Q_N} \cdot i_{cell,k} + w_{SOC,k} \\ \frac{T^\alpha(\text{SOC}_k)}{Q(\text{SOC}_k)} (i_{cell,k} - \frac{u_{RQ,k}}{R(\text{SOC}_k)}) - \Lambda_{k|z} + w_{RQ,k} \end{pmatrix} \\ &=: \mathbf{f}_{cell}(\mathbf{x}_{cell,i}, i_{cell})_k \end{aligned} \quad (12)$$

$$\begin{aligned} \mathbf{y}_{cell,i,k} &:= u_{RQ,k} + R_0(\text{SOC}_k) i_{cell,k} + \text{OCV}(\text{SOC}_k) + v_{cell,k} \\ &=: \mathbf{g}_{cell}(\mathbf{x}_{cell,i}, i_{cell})_k. \end{aligned} \quad (13)$$

### 3.2 Model of a Branch

A serial connection of  $s$  single cells like in Fig. 3 is called a ‘branch’. Hereby, an additional serial resistance  $R_c$  is included to consider connection and wire resistances. Therefore,  $R_c$  can differ in every branch, but is assumed to be known.

As the cells are serially connected, the cell currents are identical in every cell and the cell voltages sum up to a total voltage

$$u_{total,b} = \sum_{r=1}^s u_{cell,b,r} + R_{c,b} i_{branch,b} \quad (14)$$

whereas  $b$  denotes the index of the branch. The model for

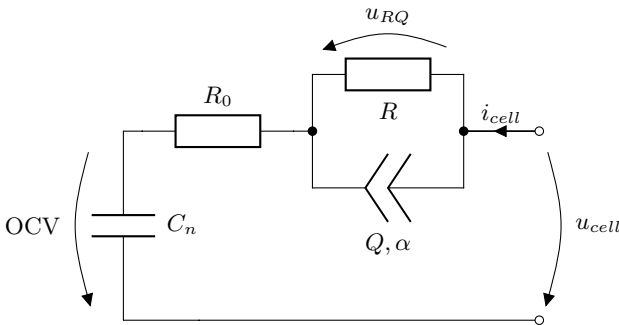


Figure 1: 1-RQ equivalent circuit model of a Li-ion cell

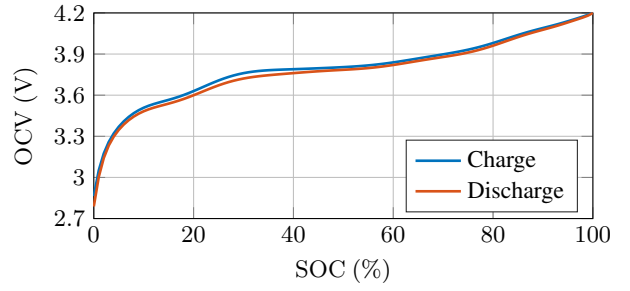


Figure 2: Open Circuit Voltage of a Li-ion Polymer Battery Cell (Type SLPB 834374H, Manufacturer Kokam)

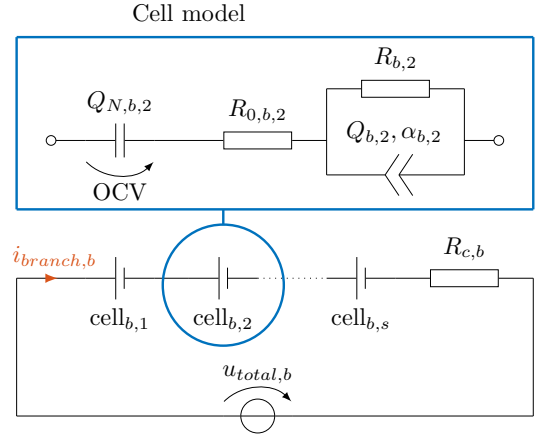


Figure 3: Serial connection of  $s$  single cells in one branch

one specific branch  $b$  results cell-wise as

$$\begin{aligned} \mathbf{x}_{branch,b,k+1} &:= \begin{pmatrix} \mathbf{x}_{cell,b,1} \\ \vdots \\ \mathbf{x}_{cell,b,s} \end{pmatrix}_{k+1} = \begin{pmatrix} \text{SOC}_{b,1} \\ u_{RQ,b,1} \\ \vdots \\ \text{SOC}_{b,s} \\ u_{RQ,b,s} \end{pmatrix}_{k+1} \\ &= \begin{pmatrix} \mathbf{f}_{cell}(\mathbf{x}_{cell,b,1}, i_{branch,b}) \\ \vdots \\ \mathbf{f}_{cell}(\mathbf{x}_{cell,b,s}, i_{branch,b}) \end{pmatrix}_k \end{aligned} \quad (15)$$

$$=: \mathbf{f}_{branch}(\mathbf{x}_{branch,b}, i_{branch,b})_k \quad (16)$$

$$\begin{aligned} \mathbf{y}_{branch,b,k} &:= \begin{pmatrix} \mathbf{g}_{cell}(\mathbf{x}_{cell,b,1}, i_{branch,b}) \\ \vdots \\ \mathbf{g}_{cell}(\mathbf{x}_{cell,b,s}, i_{branch,b}) \end{pmatrix}_k \end{aligned} \quad (17)$$

$$=: \mathbf{g}_{branch}(\mathbf{x}_{branch,b}, i_{branch,b})_k. \quad (18)$$

### 3.3 Model of a Pack

Connecting  $p$  branches in parallel and assuming that all branches are of the same size  $s$  yields a  $p \times s$  sized battery pack. An arrangement as depicted in Fig. 4 results. The resulting discrete-time state vector for the overall bat-

$$\begin{aligned}
0 &= \sum_{r=1}^s (\text{OCV}_{b,r} - \text{OCV}_{b-1,r}) + \sum_{r=1}^s (u_{RQ,b,r} - u_{RQ,b-1,r}) + \left( \sum_{r=1}^s R_{0,b,r} + R_{c,b} \right) (i_{m,b} - i_{m,b+1}) \\
&\quad - \left( \sum_{r=1}^s R_{0,b-1,r} + R_{c,b-1} \right) (i_{m,b-1} - i_{m,b}) \\
i_{branch,b,k} &= - \frac{\sum_{r=1}^s (\text{OCV}_{b,r} - \text{OCV}_{b-1,r}) + \sum_{r=1}^s (u_{RQ,b,r} - u_{RQ,b-1,r}) - \left( \sum_{r=1}^s R_{0,b-1,r} + R_{c,b-1} \right) (i_{m,b-1} - i_{m,b})}{\sum_{r=1}^s R_{0,b,r} + R_{c,b}} \Big|_k \\
&=: h_b(i_{m,b}, i_{m,b-1}, \mathbf{x}_b, \mathbf{x}_{b-1})_k \quad \forall b = 2, \dots, p-1
\end{aligned} \tag{23}$$

$$\tag{24}$$

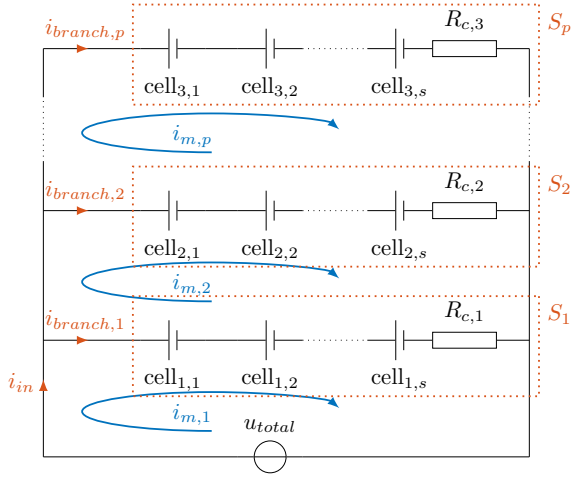


Figure 4: Mesh currents and decomposition of a large-scale system into  $p$  subsystems containing  $s$  cells each

tery pack is given branch-wise by

$$\mathbf{x}_{pack,k} = \begin{pmatrix} \mathbf{x}_{branch,1} \\ \vdots \\ \mathbf{x}_{branch,p} \end{pmatrix}_k, \quad \mathbf{y}_{pack,k} = \begin{pmatrix} \mathbf{y}_{branch,1} \\ \vdots \\ \mathbf{y}_{branch,p} \end{pmatrix}_k. \tag{19}$$

The nonlinear state-space representation of the whole  $p \times s$  sized battery pack then follows

$$\mathbf{x}_{pack,k+1} = \begin{pmatrix} \mathbf{f}_{branch}(\mathbf{x}_{branch,1}, i_{branch,1}) \\ \vdots \\ \mathbf{f}_{branch}(\mathbf{x}_{branch,p}, i_{branch,p}) \end{pmatrix}_k, \tag{20}$$

$$\mathbf{y}_{pack,k} = \begin{pmatrix} \mathbf{g}_{branch}(\mathbf{x}_{branch,1}, i_{branch,1}) \\ \vdots \\ \mathbf{g}_{branch}(\mathbf{x}_{branch,p}, i_{branch,p}) \end{pmatrix}_k. \tag{21}$$

### 3.4 Model of Branch Currents

The branch currents  $i_{branch,1}, \dots, i_{branch,p}$  used in the pack model in (20) and (21) are not equal in practice which is discussed in [15, 16, 33]. Some reasons are manufacturing tolerances, aging, and different initial SOC. There-

fore, the cell parameters are not identical and the connection resistances  $R_{c,b}$  differ as well. So, all branch currents have to be determined individually.

The most common way to determine the branch currents is to measure them by an amperemeter. The disadvantage is that this method is expensive, energy consuming, and influences the circuit [2, 18].

An alternative way of determining the branch currents for simulation purposes is proposed in [13, 33]. Instead of measuring the branch currents, a battery model is used to calculate their present value in every time step. Using mesh currents as shown in Fig. 4, the authors set up a simulation model. Evaluating the voltages in every mesh, the occurring branch currents can be calculated numerically. As this model-based approach worked well for the simulation of a battery pack, it will be extended and adapted for real-time current and SOC estimation in this paper.

According to [13, 33] and Kirchoff's voltage law [34] the branch currents  $i_{branch,b}$  can be calculated using mesh currents

$$i_{branch,b} = \begin{cases} i_{m,b} - i_{m,b+1} & \text{if } b \neq p \\ i_{m,b} & \text{if } b = p. \end{cases} \tag{22}$$

These mesh currents  $i_{m,b}$  are defined clockwise and are depicted by blue arrows in Fig. 4. With (22) and (23) the mesh current  $i_{m,b+1}$  for mesh  $b+1$  can be calculated each time step  $k$ .

Combining (22) and (23) yields (24) which calculates the branch currents directly. For the special case  $i_{branch,1}$ , equation (24) differs slightly as the measured voltage  $u_{total}$  has to be considered in the following way:

$$\begin{aligned}
i_{branch,1} &= \frac{u_{total} - \sum_{r=1}^s \text{OCV}_{1,r} - \sum_{r=1}^s u_{RQ,1,r}}{\sum_{r=1}^s R_{0,1,r} + R_{c,1}} \\
&= i_{m,1} - i_{m,2} =: h_1(i_{in}, u_{total}, \mathbf{x}_1)_k, \tag{25}
\end{aligned}$$

whereas the first mesh current corresponds to the battery pack load current  $i_{m,1} = i_{in}$  as depicted in Fig. 4 which is assumed to be the only measured current in this model. Please note that due to a concise representation of the current equations, the explicit notation of the SOC-dependency of the model parameters has been suppressed.

### 3.5 Choice of Subsystems

Since the focus of this paper is to implement a cascaded system structure with an unidirectional communication, the pack has to be split up into smaller subsystems. In this paper we suggest that every branch represents a single subsystem which is a natural division of the system because (20) and (21) are already partitioned branch-wise. Therefore, the state vector of a single subsystem  $S_a$  corresponds to the branch states and the output vector corresponds to the branch outputs

$$\mathbf{x}_{S,a} = \mathbf{x}_{branch,a}, \quad \mathbf{y}_{S,a} = \mathbf{y}_{branch,a} \quad \forall a = 1, \dots, p. \quad (26)$$

The resulting system with its  $p$  subsystems and mesh currents is shown in Fig. 4. It can be seen using (20) - (25) and in [33] that the dependency between the battery branches can be described by the branch or mesh currents, respectively. As discussed in Sec. 3.4 the branch current  $i_{branch,a}$  following (24) is a function of the states, the mesh currents and the resistances of the subsystems  $S_a$  and  $S_{a-1}$ . Therefore, the proposed model using mesh currents is suitable for a cascaded estimation approach because only an unidirectional information flow is required for a local computation.

## 4 STATE OF CHARGE AND CURRENT ESTIMATION

In this section, we describe the model-based SOC and current estimation of the battery pack model of Sec. 3.3 - 3.5. The algorithm consists of two main parts, the branch current calculation and the state estimation, both using only measurements of the total voltage  $u_{total}$ , each cell's voltage  $u_{cell}$  and the total current  $i_{in}$ . The third section describes the communication between the particular subsystems and the program flow.

### 4.1 Estimation of Branch Currents

In Sec. 3.4 the model-based calculation of branch currents has been introduced and motivated. For a model-based branch current estimation, we propose the usage of (24) and (25) for each subsystem  $S_a$  separately, because we want to calculate the estimations locally. As discussed, we need information about the states and the resistances of both subsystems  $S_a$  and  $S_{a-1}$ . The resistances and their characteristic  $R_c$  and  $R_0$ (SOC) as well as the OCV-SOC characteristic are assumed to be known as before. The states  $u_{RQ}$  and SOC of both subsystems are estimated by the CFKF which is presented in the next section. The required information from subsystem  $S_{a-1}$ , i.e. the estimated states and the resistances, is communicated to system  $S_a$ . Then, all relevant parameters are known for the calculation of  $i_{branch,a}$  in subsystem  $S_a$ .

For the calculation of the branch current  $i_{branch,k+1}$  at the next time step  $k+1$ , we use the predicted states  $\hat{\mathbf{x}}_{k+1}^- (i_{branch,k})$  of the Kalman filter because it depends only on the branch current of the current time step  $k$ . The filtered states are a function of the branch current  $\hat{\mathbf{x}}_k^+ (i_{branch,k})$  of the same time step  $k$  and, therefore, cannot be used which can be seen in (28) and (31). In accordance with (24), (25) and using the predicted states, the

branch currents result also as estimated variables:

$$\hat{i}_{branch,a,k} = \begin{cases} h_1(i_{in}, u_{total}, \hat{\mathbf{x}}_{S,1}^-)_k & a = 1 \\ \hat{i}_{m,a,k} & a = p \\ h_a(\hat{i}_{m,a}, \hat{i}_{m,a-1}, \hat{\mathbf{x}}_{S,a}^-, \hat{\mathbf{x}}_{S,a-1}^-)_k & \text{else.} \end{cases} \quad (27)$$

Again, for the first subsystem the measured variables  $u_{total}$  and  $i_{in}$  have to be considered as in (25). So the branch currents  $\hat{i}_{branch,a}$  can be calculated for all  $a = 1, \dots, p$  recursively using only the parameters from the branches  $S_a$  and  $S_{a-1}$ . Therefore, a cascaded system structure as in Fig. 5 results.

### 4.2 Cascaded Fractional Kalman Filter

In this section, a cascaded fractional Kalman filter (CFKF) for local state estimation of the branch-wise subsystem structure is proposed. We already discussed in Sec. 3.4 that the coupling between the subsystems can be described by the branch or mesh currents, respectively. Since the branch current is calculated separately as presented in Sec. 4.1, the explicit dependency of other subsystems is already included in the branch current and the formulas simplify compared to [25]. For the current calculation, we treat the predicted states as deterministic variables. This is much easier to handle as the covariances of the estimated states have not to be communicated between the subsystems. Moreover, it was shown in [25] that deterministic and stochastic treatment of the estimated states yield comparable results. Also, measured branch currents are often treated as deterministic variables as well [2].

The CFKF algorithm from [25], adapted for the battery model and applied for a particular subsystem  $a$  results then as follows:

Prediction equations:

$$\hat{\mathbf{x}}_{S,a,k+1}^- = \mathbf{f}_{branch}(\hat{\mathbf{x}}_{S,a}^+, \hat{i}_{branch})_k, \quad (28)$$

$$\mathbf{P}_{a,k+1}^- = (\mathbf{A}_{a,k} + \mathbf{\Gamma}_{a,1,k})\mathbf{P}_{a,k}^+ (\mathbf{A}_{a,k} + \mathbf{\Gamma}_{a,1,k})^T + \mathbf{Q}_{a,k} + \sum_{j=2}^z \mathbf{\Gamma}_{a,j,k} \mathbf{P}_{a,k-j+1}^+ \mathbf{\Gamma}_{a,j,k}^T. \quad (29)$$

Current estimation:

$$\hat{i}_{branch,a,k} = \begin{cases} h_1(i_{in}, u_{total}, \hat{\mathbf{x}}_{S,1}^-)_k & a = 1 \\ \hat{i}_{m,a,k} & a = p \\ h_a(\hat{i}_{m,a}, \hat{i}_{m,a-1}, \hat{\mathbf{x}}_{S,a}^-, \hat{\mathbf{x}}_{S,a-1}^-)_k & \text{else.} \end{cases} \quad (30)$$

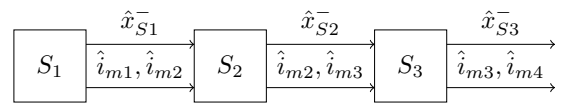


Figure 5: Communication flow between subsystems in cascaded structure

Correction equations:

$$\hat{\mathbf{x}}_{S,a,k}^+ = \hat{\mathbf{x}}_{S,a,k}^- + \mathbf{K}_{a,k}(\mathbf{y}_{S,a,k} - \mathbf{g}_{branch}(\hat{\mathbf{x}}_{S,a,k}^-, \hat{i}_{branch,k})), \quad (31)$$

$$\mathbf{P}_{a,k}^+ = (\mathbf{I} - \mathbf{K}_{a,k}\mathbf{C}_{a,k})\mathbf{P}_{a,k}^-(\mathbf{I} - \mathbf{K}_{a,k}\mathbf{C}_{a,k})^T + \mathbf{K}_{a,k}\mathbf{R}_a\mathbf{K}_{a,k}^T, \quad (32)$$

$$\mathbf{K}_{a,k} = \mathbf{P}_{a,k}^-\mathbf{C}_{a,k}^T(\mathbf{C}_{a,k}\mathbf{P}_{a,k}^-\mathbf{C}_{a,k}^T + \mathbf{R}_{a,k})^{-1}, \quad (33)$$

where  $\mathbf{x}_{S,a}^-$  are the predicted states,  $\mathbf{x}_{S,a}^+$  are the updated states, and  $\mathbf{y}_{S,a}$  are the outputs of subsystem  $S_a$ .  $\mathbf{P}_{a,k}^-$  is the predicted and  $\mathbf{P}_{a,k}^+$  the updated estimation error covariance matrix,  $\mathbf{Q}_{a,k} = E\{\mathbf{w}_k\mathbf{w}_k^T\}_a$  is the measurement noise covariance matrix and  $\mathbf{R}_{a,k} = E\{\mathbf{v}_k\mathbf{v}_k^T\}_a$  is the system noise covariance matrix of subsystem  $S_a$ . The nonlinearities of the system are treated by linearization for the calculation of the covariance matrices, identical to an extended Kalman filter [6]. Therefore, the Jacobian matrices  $\mathbf{A}_{a,k}$  and  $\mathbf{C}_{a,k}$  are given by

$$\mathbf{A}_{a,k} = \left[ \frac{\partial \mathbf{f}_{branch}(\mathbf{x}_{S,a}, i)}{\partial \mathbf{x}_{S,a}} \right]_{\mathbf{x}_{S,a} = \hat{\mathbf{x}}_{S,a,k}^+, i = \hat{i}_{branch,k}} \quad (34)$$

$$\mathbf{C}_{a,k} = \left[ \frac{\partial \mathbf{g}_{branch}(\mathbf{x}_{S,a}, i)}{\partial \mathbf{x}_{S,a}} \right]_{\mathbf{x}_{S,a} = \hat{\mathbf{x}}_{S,a,k}^-, i = \hat{i}_{branch,k}} \quad (35)$$

### 4.3 Communication Procedure and Discussion

Summarizing, the algorithm consists of two main parts that are tightly cooperating with each other. On the one hand the CFKF estimates the state vector and on the other hand the mesh equations are solved for providing the branch current. This calculation is done locally at each subsystem. Therefore, the subsystems have to exchange necessary information. This exchange can be realized via a communication line. An overview of the communication processes and of the program flow is presented in Fig. 6.

In this way, all branch currents can be calculated recursively. The cascaded scaling of the system causes that estimated states are not handed over to every single subsystem but only to the following one. Therefore, the communication effort is comparatively low, even when the number of battery branches per pack increases. However, the communication among a huge number of subsystems may become difficult because of time delays depending on the realization of the communication. A further advantage is the possibility to use local processing units to execute the calculations in each subsystem. Hence, a split up of computing power can be achieved. Furthermore, the number of current measurements is reduced considerably. For this reason, the overall costs reduce significantly.

## 5 MEASUREMENT SETUP AND RESULTS

For the validation of the functionality of the proposed model and algorithm in practice, a real-world experiment was set up. The setup consists of an A/D-board DS2004 from dSpace for cell voltage measurements  $u_{cell}$  of each

cell and total voltage measurement  $u_{total}$  and a current source BOP20-20M from Kepco for measurement and control of the load current  $i_{in}$  which is shown in Fig. 7. For comparison reasons each branch contains also a highly accurate 34410A multimeter from Keysight Technologies to validate the model-based calculation of the branch currents with the measured branch currents  $i_c$ . The battery pack under investigation consists of 3 branches containing 3 cells each. The additional resistances  $R_c$  differ in each branch. They have been identified to

$$R_{c,1} = 540 \text{ m}\Omega, R_{c,2} = 610 \text{ m}\Omega, R_{c,3} = 650 \text{ m}\Omega. \quad (36)$$

The initial states of the branches have been determined using cell voltage measurements of each cell before wiring the cells to a pack, after a rest time of  $t = 1000$  s. Assuming that all  $u_{RQ} \approx 0$  V after the rest time, the initial SOCs have been identified using the OCV-SOC relation. The initial states for the three branches are

$$\begin{aligned} \mathbf{x}_{branch,1,0} &= (95.3\% \ 0 \text{ V} \ 85.5\% \ 0 \text{ V} \ 74.9\% \ 0 \text{ V})^\top, \\ \mathbf{x}_{branch,2,0} &= (90.5\% \ 0 \text{ V} \ 80.8\% \ 0 \text{ V} \ 69.4\% \ 0 \text{ V})^\top, \\ \mathbf{x}_{branch,3,0} &= (85.6\% \ 0 \text{ V} \ 76.1\% \ 0 \text{ V} \ 64.6\% \ 0 \text{ V})^\top. \end{aligned}$$

For the CFKF algorithm we use a sampling time  $T = 0.1$  s, a memory length  $l = 250$ , covariance matrices

$$\mathbf{Q}_{a,k} = \text{diag} [10^{-5} \%, 5 \cdot 10^{-4} \text{ V}^2, 10^{-5} \%, 5 \cdot 10^{-4} \text{ V}^2, 10^{-5} \%, 5 \cdot 10^{-4} \text{ V}^2] \quad \forall a, k \quad (37)$$

$$\mathbf{R}_{a,k} = \text{diag} [2.8391 \cdot 10^{-8} \text{ V}^2, 2.8391 \cdot 10^{-8} \text{ V}^2, 2.8391 \cdot 10^{-8} \text{ V}^2] \quad \forall a, k \quad (38)$$

$$\mathbf{P}_{a,0} = \text{diag} [100 \%, 100 \text{ V}^2, 100 \%, 100 \text{ V}^2, 100 \%, 100 \text{ V}^2] \quad \forall a \quad (39)$$

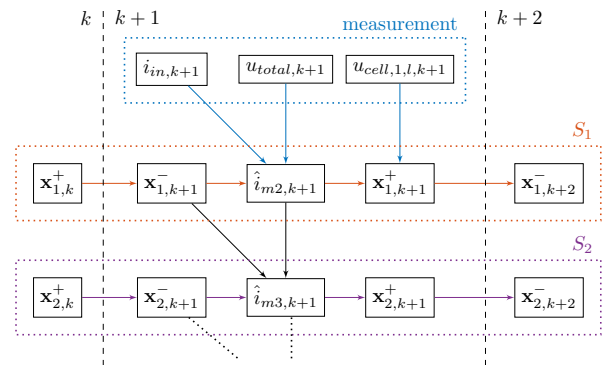


Figure 6: Procedure and communication order in the cascaded algorithm. Orange and purple arrows show the processing order within the subsystems, blue arrows show measured values and black arrows depict the information flow between subsystems.

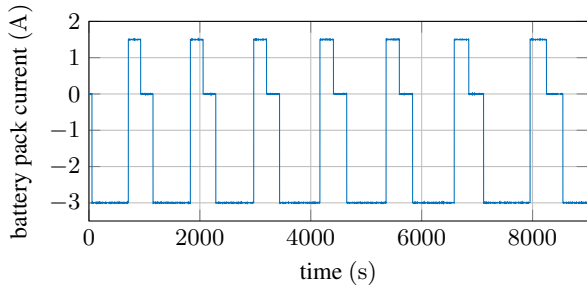


Figure 7: Input current  $i_{in}$  for the measurement setup

and the initial SOCs of the filter algorithm as

$$\begin{aligned}\hat{\mathbf{x}}_{branch,1,0} &= (93.3\% \ 0 \text{ V} \ 88.5\% \ 0 \text{ V} \ 79.9\% \ 0 \text{ V})^\top, \\ \hat{\mathbf{x}}_{branch,2,0} &= (93.5\% \ 0 \text{ V} \ 77.8\% \ 0 \text{ V} \ 73.4\% \ 0 \text{ V})^\top, \\ \hat{\mathbf{x}}_{branch,3,0} &= (81.6\% \ 0 \text{ V} \ 81.1\% \ 0 \text{ V} \ 63.6\% \ 0 \text{ V})^\top\end{aligned}$$

which have slight, randomly chosen deviations to the true states. Note that we parametrized only one of the cells of the pack and, therefore, the CFKF uses identical parameters for all cells, although in practice the cells may have different parameters.

Exemplary results of the experiment are shown in Fig. 8 and in Fig. 9. Fig. 8 shows the estimated branch currents  $\hat{i}_{branch}$  by the CFKF as well as the measured branch currents  $i_c$  by the Keysight multimeters. It can be seen that there are only small differences between the currents. The maximum difference of  $|\hat{i}_{branch,a,k} - i_{c,a,k}|, \forall a, k$  is smaller than 70 mA in this experiment. As a result, the current estimation can compete with the multimeter.

In Fig. 9 the estimated SOCs of the CFKF are shown exemplarily for branch 2 as well as the corresponding SOCs which are calculated by a current integration using (7) and the measured branch currents  $i_c$ . It can be seen that the states can be estimated accurately even though the filter is not correctly initialized and the parameters of all cells have been chosen identically. The difference of the estimated SOCs to the SOCs determined by the current integration is at all times for all branches smaller than the maximum initial difference of 5%.

## 6 CONCLUSION

In this paper, we presented a nonlinear variable fractional battery cell model and extended it to a battery pack model. This model uses mesh currents to describe the coupling between the branches and for the branch current calculation. It has been shown that this model is suitable for a cascaded estimation approach which estimates the states of each cell of the battery pack model as well as each branch current. The results show that the estimated branch currents match with the measured ones although the parameters have been identified only for one cell and all other cells may have slightly different parameters. The state estimation achieves good results as expected because the current estimation works correctly and the Kalman filter algorithm is robust with respect to measurement, parameter, and linearization errors.

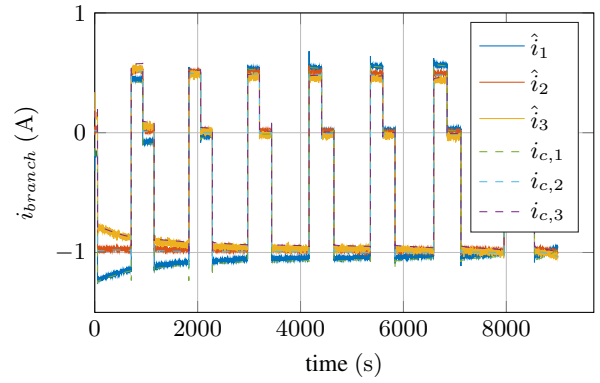


Figure 8: Comparison of estimated branch currents  $\hat{i}$  and measured branch currents  $i_c$

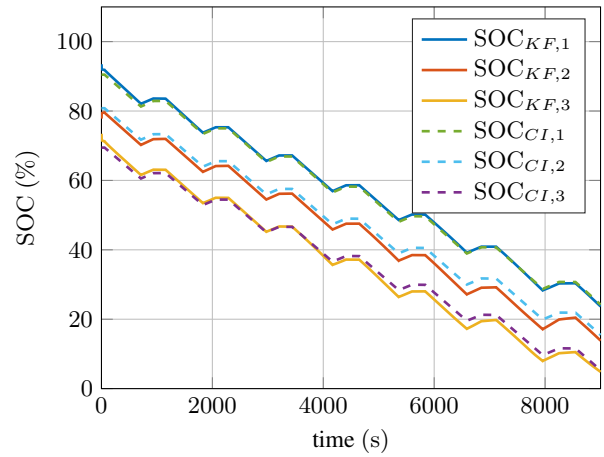


Figure 9: Estimated SOCs of branch 2 of the CFKF compared to an integration of the measured current  $i_c$

We also discussed the division of the system into subsystems in that way that each branch represents one subsystem. This approach achieves scalability and also obtains small and simple subsystems which are easier to handle, especially for large-scale systems. These subsystems only need an unidirectional communication between neighbouring subsystems. However, a division into subsystems is not binding since the algorithm can also be implemented on a single processor. Furthermore, it is also not mandatory to use a fractional order battery model because one can simply adopt integer order models by setting  $\alpha = 1$ . Summarizing, the CFKF for the cascaded state and current estimation has various advantages, e.g. shared computation costs between the subsystems and reduced measurement effort with consistent accuracy. Further improvements of the CFKF can be made by considering the covariances of the states for the current estimation, by identifying the parameters of each cell individually, and by increasing the buffer length of the Grünwald-Letnikov sum.

## REFERENCES

- [1] W.-Y. Chang, “The state of charge estimating methods for battery: A review,” *ISRN Applied Mathematics*, pp. 1–7, 2013.

- [2] W. Waag, C. Fleischer, and D. U. Sauer, "Critical review of the methods for monitoring of lithium-ion batteries in electric and hybrid vehicles," *Journal of Power Sources*, vol. 258, pp. 321–339, 2014.
- [3] Q. Zhu, N. Xiong, M.-L. Yang, R.-S. Huang, and G.-D. Hu, "State of charge estimation for lithium-ion battery based on nonlinear observer: an  $H_\infty$  method," *Energies*, vol. 10, no. 5, p. 679, 2017.
- [4] Y. Ma, X. Zhou, B. Li, and H. Chen, "Fractional modeling and SOC estimation of lithium-ion battery," *IEEE/CAA Journal of Automatica Sinica*, vol. 3, no. 3, pp. 281–287, 2016.
- [5] J. Francisco, J. Sabatier, L. Lavigne, F. Guillemard, M. Moze, M. Tari, M. Merveillaut, and A. Noury, "Lithium-ion battery state of charge estimation using a fractional battery model," in *International Conference on Fractional Differentiation and Its Applications (ICFDA)*. IEEE, 2014, pp. 1–6.
- [6] M. Kupper, C. Funk, M. Eckert, and S. Hohmann, "Fractional extended and unscented Kalman filtering for state of charge estimation of lithium-ion batteries," in *American Control Conference (ACC)*. IEEE, 2018.
- [7] B. Wang, Z. Liu, S. E. Li, S. J. Moura, and H. Peng, "State-of-charge estimation for lithium-ion batteries based on a nonlinear fractional model," *IEEE Transactions on Control Systems Technology*, vol. 25, no. 1, pp. 3–11, 2017.
- [8] M. Eckert, L. Kölsch, and S. Hohmann, "Fractional algebraic identification of the distribution of relaxation times of battery cells," in *Conference on Decision and Control (CDC)*. IEEE, 2015, pp. 2101–2108.
- [9] R. Xiao, J. Shen, X. Li, W. Yan, E. Pan, and Z. Chen, "Comparisons of modeling and state of charge estimation for lithium-ion battery based on fractional order and integral order methods," *Energies*, vol. 9, no. 3, p. 184, 2016.
- [10] J. Sabatier, M. Merveillaut, J. M. Francisco, F. Guillemard, and D. Porcelatto, "Fractional models for lithium-ion batteries," in *2013 European Control Conference (ECC)*, 2013.
- [11] M. Eckert, M. Kupper, and S. Hohmann, "Functional fractional calculus for system identification of battery cells," *at - Automatisierungstechnik*, vol. 62, no. 62, pp. 272–281, 2014.
- [12] J. Illig, T. Chrobak, M. Ender, J. P. Schmidt, D. Klotz, and E. Ivers-Tiffée, "Studies on  $LiFePO_4$  as cathode material in Li-ion batteries," *ECS Transactions*, vol. 28, no. 30, pp. 3–17, 2010.
- [13] T. Bruen and J. Marco, "Modelling and experimental evaluation of parallel connected lithium ion cells for an electric vehicle battery system," *Journal of Power Sources*, vol. 310, pp. 91–101, 2016.
- [14] J.-M. Tarascon and M. Armand, "Issues and challenges facing rechargeable lithium batteries," in *Materials For Sustainable Energy*. World Scientific, 2011, pp. 171–179.
- [15] N. Yang, X. Zhang, B. Shang, and G. Li, "Unbalanced discharging and aging due to temperature differences among the cells in a lithium-ion battery pack with parallel combination," *Journal of Power Sources*, vol. 306, pp. 733–741, 2016.
- [16] H. Dai, X. Wei, Z. Sun, J. Wang, and W. Gu, "Online cell SOC estimation of Li-ion battery packs using a dual time-scale Kalman filtering for EV applications," *Applied Energy*, vol. 95, pp. 227–237, 2012.
- [17] L. Zhong, C. Zhang, Y. He, and Z. Chen, "A method for the estimation of the battery pack state of charge based on in-pack cells uniformity analysis," *Applied Energy*, vol. 113, pp. 558–564, 2014.
- [18] C. Y. Chun, J. Baek, G.-S. Seo, B. Cho, J. Kim, I. K. Chang, and S. Lee, "Current sensor-less state-of-charge estimation algorithm for lithium-ion batteries utilizing filtered terminal voltage," *Journal of Power Sources*, vol. 273, pp. 255–263, 2015.
- [19] M.-S. Wu, C.-Y. Lin, Y.-Y. Wang, C.-C. Wan, and C. Yang, "Numerical simulation for the discharge behaviors of batteries in series and/or parallel-connected battery pack," *Electrochimica acta*, vol. 52, no. 3, pp. 1349–1357, 2006.
- [20] F. Sun, X. Hu, Y. Zou, and S. Li, "Adaptive unscented kalman filtering for state of charge estimation of a lithium-ion battery for electric vehicles," *Energy*, vol. 36, no. 5, pp. 3531–3540, 2011.
- [21] P. Hilgers and C. Ament, "Distributed and decentralised estimation of non-linear systems," in *International Conference on Control Applications (CCA)*. IEEE, 2010, pp. 328–333.
- [22] A. G. O. Mutambara and H. F. Durrant-Whyte, "Distributed decentralized robot control," in *American Control Conference*. IEEE, 1994, pp. 2266–2267.
- [23] M. Kupper, I. Sesar Gil, and S. Hohmann, "Distributed and decentralized state estimation of fractional order systems," in *American Control Conference (ACC)*. IEEE, 2016, pp. 2765–2771.
- [24] Z. Lendek, R. Babuska, and B. D. Shutter, "Distributed Kalman filtering for cascaded systems," *Engineering applications of artificial intelligence*, vol. 21, pp. 457 – 569, 2008.
- [25] M. Kupper, I. Sesar Gil, and S. Hohmann, "Distributed and decentralized Kalman filtering for cascaded fractional order systems," in *American Control Conference (ACC)*. IEEE, 2017, pp. 5223–5230.
- [26] D. Valério and J. Sá da Costa, "Variable order fractional controllers," *Asian Journal of Control*, vol. 15, no. 3, pp. 648–657, 2013.
- [27] D. Sierociuk and A. Dzieliński, "Fractional Kalman filter algorithm for the states, parameters and order of fractional system estimation," *International Journal of Applied Mathematics and Computer Science*, vol. 16, no. 1, pp. 129 – 140, 2006.
- [28] C. A. Monje, Y. Chen, B. M. Vinagre, D. Xue, and V. Feliu-Batlle, *Fractional-order systems and controls: fundamentals and applications*. Springer Science & Business Media, 2010.
- [29] J. Sabatier, C. Farges, and J.-C. Trigeassou, "Fractional systems state space description: some wrong ideas and proposed solutions," *Journal of Vibration and Control*, vol. 20, no. 7, pp. 1076–1084, 2014.
- [30] C. F. Lorenzo and T. T. Hartley, *Initialized fractional calculus*. NASA, Glenn Research Center, 2000.
- [31] M. Mastali, J. Vazquez-Arenas, R. Fraser, M. Fowler, S. Afshar, and M. Stevens, "Battery state of the charge estimation using Kalman filtering," *Journal of Power Sources*, vol. 239, pp. 294–307, 2013.
- [32] G. L. Plett, "Extended Kalman filtering for battery management systems of LiPB-based HEV battery packs-part 2. modeling and identification," *Journal of Power Sources*, vol. 2, no. 134, pp. 262–276, 2004.
- [33] T. Bruen, J. Marco, and M. Gama, "Current variation in parallelized energy storage systems," in *Vehicle Power and Propulsion Conference (VPPC)*. IEEE, 2014, pp. 1–6.
- [34] I. D. Mayergoyz and W. Lawson, *Basic Electric Circuit Theory*. Academic Press, 1997.